JOURNAL OF Materials CHEMISTRY

MCM-41 functionalized with bipyridyl groups and its use as a support for oxomolybdenum(VI) catalysts

Carla D. Nunes,[a] Anabela A. Valente,[a] Martyn Pillinger,[a] Ana C. Fernandes,[b] Carlos C. Romão,[b] João Rocha[a] and Isabel S. Gonçalves*[a]

[a]*Department of Chemistry, University of Aveiro, Campus de Santiago, 3810-193 Aveiro, Portugal. E-mail: igoncalves@dq.ua.pt*
[b]*Instituto de Tecnologia Química e Biológica da Universidade Nova de Lisboa, Quinta do Marquês, EAN, Apt 127, 2781-901 Oeiras, Portugal*

Received 24th October 2001, Accepted 14th March 2002
First published as an Advance Article on the web 10th April 2002

The ordered mesoporous silica MCM-41 was covalently grafted with (3-chloropropyl)trimethoxysilane. Chloro substitution by the anion [4-CH_2-4′-Me-2,2′-bipyridine]$^-$ gave a ligand-silica containing *ca.* 0.3 mmol bipyridyl groups per gram. Powder X-ray diffraction and nitrogen adsorption–desorption analysis demonstrated that the textural characteristics of the support were preserved during the grafting experiments and that the channels remained accessible, despite sequential reductions in surface area, pore volume and pore size. The coupling reactions were monitored by ^{29}Si MAS NMR and ^{13}C CP MAS NMR spectroscopy. Bipyridyl-functionalized MCM-41 exhibits a high encapsulating ability, as evidenced by its interaction with a dichloromethane solution of $MoO_2Cl_2(THF)_2$. A material with a metal loading of 8.3 mass% was obtained. Molybdenum K-edge EXAFS analysis could not substantiate the formation of a tethered complex of the type MoO_2Cl_2(N–N), but instead indicated the formation of unidentate-bridged entities of the type [O_2Mo–X–MoO_2] with a metal–metal separation of 3.28 Å. The molybdenum-containing MCM was active as a catalyst for the epoxidation of cyclooctene by *tert*-butyl hydroperoxide. However, this activity is due, at least in part, to leached molybdenum species in solution.

Introduction

Amorphous silica, alumina and other inorganic oxides have found widespread use as supports for the immobilization of catalytically active sites and photo- and electro-active species.[1] The materials present hydroxyl-covered surfaces that facilitate derivatization. In order to functionalize a silica surface, for example, a molecule containing a ligand group, or a group that may be readily converted to a ligand group, is reacted with the surface silanol groups. One approach is to use silane coupling agents.[2] Howell and co-workers used functional alkoxysilanes to anchor PPh_2, CN, NH_2, pyridine and cyclopentadiene ligands, amongst others.[3–5] The resulting ligand-silicas were used to prepare a range of supported complexes of rhodium, cobalt, nickel, palladium, platinum, iridium and ruthenium. More recently, Angelici and co-workers reported the hydrogenation of arenes under mild conditions using rhodium bipyridyl complexes tethered to a silica-supported palladium heterogeneous catalyst.[6] The precursor rhodium complex used was of the type $[Rh(COD)(L)]BF_4$, where L = 2,2′-bipyridyl-3,3′-[$C(O)NH(CH_2)_3Si(OC_2H_5)_3$]$_2$. The important feature of this complex is that the chelating ligand binds strongly to the metal ion and therefore leaching of the metal ion should be reduced when the ligand is tethered to a support.

In the past decade micelle-templated inorganic oxides have emerged as very promising support materials owing to their unique textural properties (high surface area and pore volume coupled with narrow pore size distributions).[7] The most studied example is the hexagonally-ordered material MCM-41.[8] The inclusion chemistry of ordered mesoporous oxides like MCM-41 has been investigated for many purposes, particularly catalytic applications.[9–11] Transition metal–bipyridine complexes have so far been incorporated in such materials by either direct incipient-wetness impregnation or ion-exchange.[12,13] For example, manganese 2,2′-bipyridine (bpy) complex cations, $[Mn(bpy)_2]^{2+}$, were immobilized in MCM-41 and used as a catalyst for the oxidation of styrene by iodosylbenzene, H_2O_2 and *tert*-butyl hydroperoxide (TBHP).[12] The approach described in the present paper is to functionalize MCM-41 with covalently tethered unsymmetrical 4,4′-dialkyl-2,2′-bipyridyl groups. The interaction of the ligand-silica with the complex $MoO_2Cl_2(THF)_2$ was then investigated, with the intention of forming surface-bound Lewis base adducts of the type MoO_2Cl_2(N–N). All materials have been characterized by a range of techniques and the final supported Mo complex tested as a catalyst in the liquid-phase epoxidation of cyclooctene using TBHP.

Experimental

Reagents

All preparations and manipulations were carried out using standard Schlenk techniques under nitrogen. Solvents were dried by standard procedures (THF, *n*-hexane and diethyl ether with Na/benzophenone ketyl; CH_2Cl_2 and MeCN with CaH_2), distilled under nitrogen and kept over 4 Å molecular sieves (3 Å for MeCN). The precursor materials MoO_2Cl_2,[14] $MoO_2Cl_2(THF)_2$ (**1**),[15] MoO_2Cl_2(4,4′-dimethyl-2,2′-bipyridine) (**2**)[16] and lithium diisopropylamine[17] were prepared using literature procedures. 4,4′-Dimethyl-2,2′-bipyridine was purchased from Aldrich and used as received.

Characterization

Microanalyses were performed at the ITQB and the Mikroanalytische Labor of the Technical University of Munich (M. Barth and co-workers). TGA studies were performed using a Mettler TA3000 system at a heating rate of 5 K min^{-1} under a static atmosphere of air. Powder X-ray diffraction (XRD) data

were collected with a Philips X'pert diffractometer using Cu Kα radiation filtered by Ni. IR spectra were measured with a Unican Mattson Mod 7000 FTIR spectrometer using KBr pellets.

Nitrogen adsorption–desorption isotherms were measured at 77 K, using a gravimetric adsorption apparatus equipped with a CI electronic MK2-M5 microbalance and an Edwards Barocel pressure sensor. The out-gassing temperature was slowly raised (1 K min^{-1}) to 723 K for MCM-41-1 and 413 K for the modified materials (to minimize destruction of the functionalities) and maintained at that temperature overnight to a residual pressure of *ca.* 10^{-4} mbar. The specific surface areas (S_{BET}) were calculated applying the BET equation for relative pressures between 0.05 and 0.25, taking the projection area of a nitrogen molecule as 0.162 nm^2 $molecule^{-1}$. The specific total pore volume (micropore plus mesopore, V_P) was estimated from the N_2 uptake at $p/p_0 \approx 0.95$, using the liquid density of N_2 at 77 K as 0.8081 g cm^{-3}.

The pore size distribution curves (PSD – differential volume adsorbed with respect to the differential pore size per unit mass *vs.* pore radius) were computed from the desorption branch of the experimental isotherms, using a method based on the area of the pore walls.[18,19] Assuming open cylindrical pores with radius r_p and zero contact angle, and correcting for the thickness of the layer already adsorbed, r_p can be calculated by summing the Kelvin radius and the statistical average thickness (t) of the adsorbed layer.[18] The t values were derived from a standard nitrogen isotherm for nonporous hydroxylated silica, available in the literature,[20] using the Halsey equation.[18]

^{29}Si and ^{13}C solid-state NMR spectra were recorded at 79.49 and 100.62 MHz, respectively, with a (9.4 T) Bruker MSL 400P spectrometer. ^{29}Si MAS NMR spectra were recorded with 40° pulses, spinning rates 5.0–5.5 kHz and 60 s recycle delays. ^{29}Si CP MAS NMR spectra were recorded with 5.5 μs ^1H 90° pulses, 8 ms contact time, a spinning rate of 4.5 kHz and 4 s recycle delays. ^{13}C CP MAS NMR spectra were recorded with a 4.5 μs ^1H 90° pulse, 2 ms contact time, a spinning rate of 8 kHz and 4 s recycle delays. Chemical shifts are quoted in parts per million from tetramethylsilane (TMS).

Mo K-edge X-ray absorption spectra were measured at room temperature in transmission mode on beamline BM29 at the ESRF (Grenoble), operating at 6 GeV in 2/3 filling mode with typical currents of 170–200 mA. Typically, one scan was performed for each sample in the range 19.6–22.0 keV and set up to record the pre-edge at 5 eV steps and the post-edge region in 0.025–0.05 $Å^{-1}$ steps, giving a total acquisition time of *ca.* 40 min per scan. The order-sorting double Si(311) crystal monochromator was detuned to give 40% harmonic rejection. Solid samples were diluted with BN and pressed into 13 mm pellets. Air-sensitive samples were handled under an inert gas. Ionization chamber detectors were filled with Kr to give 30% absorbing I_o (incidence) and 80% absorbing I_t (transmission).

The programs EXCALIB and EXBACK (SRS Daresbury Laboratory, UK) were used in the usual manner for calibration and background subtraction of the raw data. EXAFS curve-fitting analyses, by least-squares refinement of the non-Fourier filtered k^3-weighted EXAFS data, were carried out using the program EXCURVE (version EXCURV98[21]) using fast curved wave theory.[22] Phase shifts were obtained within this program using *ab initio* calculations based on the Hedin Lundqvist/von Barth scheme.

Synthesis of the materials

MCM-41 (MCM-41-1). MCM-41 was crystallized from a gel with the molar composition $SiO_2 : 0.29Na_2O : 0.50C_{14}TMABr : 150H_2O$. Specifically, 9.9 g sodium silicate solution (8% Na_2O, 27% SiO_2, Merck) were diluted with 30 mL H_2O and added slowly to a rapidly stirred solution of 7.48 g $[(C_{14}H_{29})NMe_3]Br$ in 80 mL H_2O. A precipitate formed immediately which was stirred at ambient temperature for 30 min. Dilute sulfuric acid (2 M) was then added dropwise to adjust the pH of the gel from 12.0 to 10.0. After stirring for a further 30 min, the pH was readjusted to 10.0. The mixture was then autoclaved at 100 °C for 2 days in Teflon-lined stainless steel reaction vessels. The solid product was recovered by filtration, washed with hot water and air-dried at 60 °C. Calcination was carried out at 540 °C for 6 h to remove the surfactant MCM-41 grafted with chloropropylsilyl groups (MCM-41-2)

MCM-41 grafted with chloropropylsilyl groups (MCM-41-2). Physisorbed water was removed from calcined MCM-41-1 (2.0 g) by heating at 180 °C under vacuum (10^{-2} mbar) for 2 h. The dry material was then treated with an excess of a solution of $Cl(CH_2)_3Si(OMe)_3$ (2.0 mL) in toluene (30 mL) and the mixture stirred under reflux for 24 h. The solution was filtered off and the solid washed six times with 30 mL aliquots of dichloromethane, before drying under vacuum at room temperature for several hours. Anal. Found: C, 8.41; H, 1.88; Cl, 5.86; Si, 36.05%. IR (KBr, ν/cm^{-1}): 3008 w, 2958 m, 2850 m, 1465 m, 1238 s, 1192 s, 1085 vs, 914 m, 814 s, 697 m, 644 sh, 573 m, 458 s.

MCM-41 functionalized with 4,4′-dialkyl-2,2′-bipyridine (MCM-41-3). A solution of 4,4′-dimethyl-2,2′-bipyridine (1.5 g, 8.16 mmol) in THF (40 mL) was added to a THF solution of lithium diisopropylamine (8.0 mmol). After 2 h the orange-brown solution was cooled to −20 °C and MCM-41-2 (2.0 g) added. After 72 h, the reaction mixture was treated with ice water. The solution was filtered off and the pale rose solid washed three times with 15 mL aliquots of ethanol, three times with 15 mL aliquots of diethyl ether, and dried under vacuum at room temperature for several hours. Anal. Found: C, 13.80; H, 2.91; N, 0.81; Cl, 3.80; Si, 32.6%. IR (KBr, ν/cm^{-1}): 3455 s, 2938 m, 1637 s, 1598 m, 1554 m, 1460 m, 1438 m, 1408 m, 1383 m, 1080 vs, 954 s, 866 m, 799 s, 689 m, 554 sh, 458 s.

Immobilization of dioxomolybdenum(VI) (MCM-41-4). A suspension of MCM-41-3 (0.5 g) in CH_2Cl_2 was treated with a solution of $MoO_2Cl_2(THF)_2$ (0.3 g, 0.87 mmol) in CH_2Cl_2 (30 mL) and the mixture stirred at room temperature for 24 h. The solution was filtered off and the pale blue solid washed four times with 20 mL aliquots of CH_2Cl_2, and finally dried under vacuum at room temperature for several hours. Anal. Found: C, 11.51; H, 2.79; N, 0.68; Cl, 9.06; Mo, 8.3; Si, 26.8%. IR (KBr, ν/cm^{-1}): 2944 m, 1624 s, 1559 m, 1490 m, 1419 m, 1231 s, 1080 vs, 941 m, 911 m, 801 m, 693 m, 565 m, 462 s.

Catalytic epoxidation reactions. The liquid-phase oxidation of cyclooctene was carried out at 55 °C under air atmosphere, in a batch reactor equipped with a magnetic stirrer. The reactor was loaded with 175 mg of catalyst, 7.3 mmol cyclooctene and 11 mmol of *tert*-butyl hydroperoxide as oxidant (5.5 M in decane). Samples were withdrawn periodically and analyzed using a gas chromatograph (Varian 3800) equipped with a capillary column (DB-5, 30 m × 0.25 mm × 0.25 mm) and a flame ionization detector. The products were identified by gas chromatography–mass spectrometry (HP 5890 Series II GC; HP 5970 Series Mass Selective Detector) using He as carrier gas.

Results and discussion

Synthesis

The parent MCM-41 sample (MCM-41-1), prepared using $[(C_{14}H_{29})NMe_3]Br$ as the surfactant template, was of good quality according to powder XRD and N_2 adsorption–desorption analysis (see below). Initially, it was anticipated that the desired functionalized material could be prepared

by treating the pristine support with the adduct {4-[Si(OMe)$_3$(CH$_2$)$_4$]-4′-methyl-2,2′-bipyridine}MoO_2Cl_2. However, the preparation of the ligand 4-[Si(OMe)$_3$(CH$_2$)$_4$]-4′-methyl-2,2′-bipyridine presents considerable difficulties owing to the reactivity of the trimethoxysilyl group, *i.e.* the product always appears as a polymeric material that is difficult to characterize. The alternative approach is to derivatize MCM-41 with chloropropylsilyl groups and then to carry out subsequent reactions to construct the target immobilized species (Scheme 1). Refluxing calcined and dehydrated MCM-41-1 with a toluene solution of (3-chloropropyl)trimethoxysilane under nitrogen gave the surface-bound chloropropylsilyl groups at a loading of *ca.* 1.65 mmol g^{-1} (by elemental analysis). This corresponds to a surface coverage of about 1.2 chains per nm^2, which is similar to experimentally determined values for the concentration of free silanol groups on the surface of pristine MCM-41.[23] The C : Cl molar ratio in MCM-41-2 (4.3 : 1) suggests that methoxy groups were eliminated to form at least one Si–O–Si bond. TGA of MCM-41-2 showed a mass loss of 19.9% between 25 and 400 °C (DTG_{max} *ca.* 300 °C).

MCM-41 functionalized with bipyridyl groups was prepared by applying the method reported by Ellison and Iwamoto for the synthesis of unsymmetrical 4-alkyl-4′-methyl-2,2′-bipyridines.[17] One of the methyl groups of 4,4′-dimethyl-2,2′-bipyridine was converted with lithium diisopropylamine to –CH_2 anionic groups, and the latter subsequently caused to react with the alkyl chloride MCM-41-2. Elemental analysis indicated that the Cl content in MCM-41-3 was reduced (relative to MCM-41-2) to 1.07 mmol g^{-1} and the N content was 0.58 mmol g^{-1}. This indicates that *ca.* 21% of Cl groups in MCM-41-2 were eliminated by nucleophilic replacement to form covalently tethered bipyridine ligands (Scheme 1). In the IR spectrum, the pyridyl ring stretching vibration of MCM-41-3 appears at 1598 cm^{-1}, the corresponding band of 4,4′-dimethyl-2,2′-bipyridine at 1592 cm^{-1}.

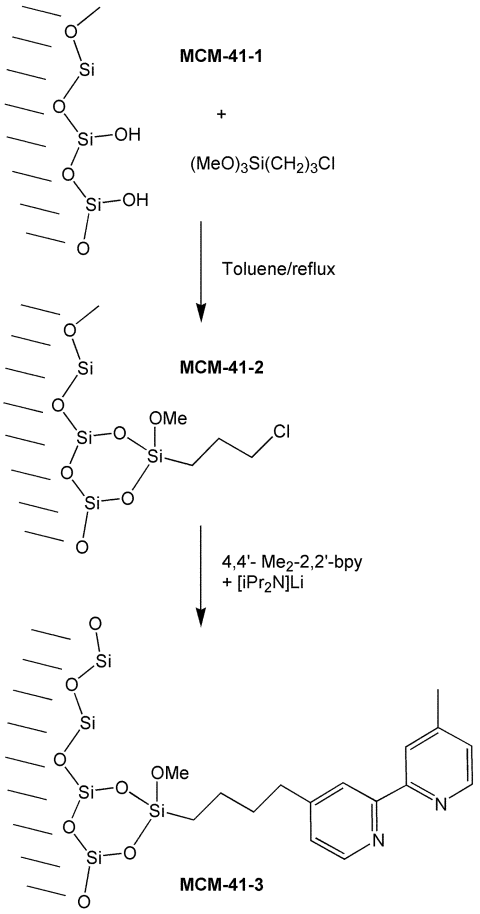

Scheme 1

Oxomolybdenum species were subsequently introduced into MCM-41-3 by pore volume impregnation of a solution of the dioxomolybdenum(VI) complex $MoO_2Cl_2(THF)_2$ in CH_2Cl_2 at room temperature. This yielded a pale blue powder (MCM-41-4) containing 8.3 mass% Mo (0.87 mmol g^{-1}) and 9.06 mass% Cl (2.55 mmol g^{-1}). If we assume that the N : Cl ratio (Cl from chloropropylsilyl groups) is unchanged in MCM-41-4 compared to MCM-41-3, it follows that the chloropropylsilyl content in MCM-41-4 corresponds to *ca.* 0.9 mmol g^{-1}. The value for the remaining Cl content (1.65 mmol g^{-1}) is consistent with retention of $MoCl_2$ stoichiometry for the guest species. Furthermore, the decrease in C content on going from MCM-41-3 to MCM-41-4 (13.8 to 11.5%) is consistent with the inclusion of 'MoO_2Cl_2' units in MCM-41-4 (0.87 mmol g^{-1}), rather than the adduct $MoO_2Cl_2(THF)_2$. The presence of a *cis*-MoO_2 unit in MCM-41-4 is confirmed by the IR spectrum which shows two bands in the expected range for the symmetric (941 cm^{-1}) and asymmetric (911 cm^{-1}) Mo=O stretching vibrations. It is worth noting at this stage that the ligand-silica MCM-41-3 exhibits a much higher encapsulating ability than MCM-41 grafted with $NC(CH_2)_2Si(OEt)_3$.[24] When the nitrile-functionalized material was treated with an excess of a solution of $MoO_2Cl_2(THF)_2$ in CH_2Cl_2, a product with only 1.0 mass% Mo was obtained.[24] This approach used in the present work is akin to that reported by Sherrington and co-workers, in which Mo^{VI} species were supported on a polybenzimidazole resin.[25]

Characterization

Powder X-ray diffraction. The powder XRD pattern of MCM-41-1 is consistent with the formation of a high quality sample (Fig. 1). Five reflections are observed in the 2θ range 2–8°, indexed assuming a hexagonal cell as (100), (110), (200), (210) and (300). The *d* value of the (100) reflection is 36.3 Å leading to a lattice constant of $a = 41.9$ Å. Five reflections are also observed for the organo-functionalized material MCM-41-2 (Fig. 1). Compared to MCM-41-1, the intensities of these reflections are almost unchanged, but there is a clear shift to higher 2θ values ($d_{100} = 35.4$ Å, $a = 40.9$ Å). Carvalho *et al.* reported a similar contraction of the hexagonal unit cell for MCM-41 grafted with (3-aminopropyl)trimethoxysilane.[26] The effect was attributed to immobilization of organosilane groups on the surface of MCM-41 channels by reaction with Si–OH groups of defect sites. This process reduces the defect sites of the material, resulting in a more dense structure with a lower *a*

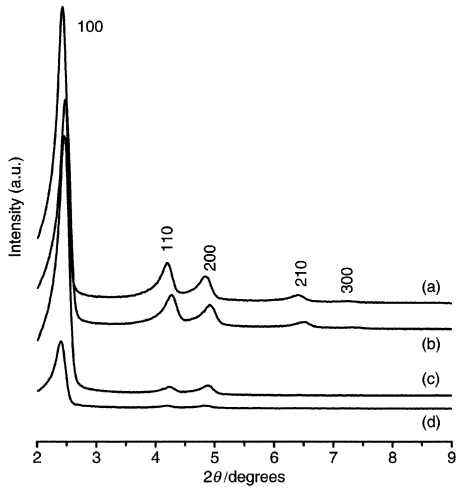

Fig. 1 Powder XRD patterns of (a) pristine MCM-41 (MCM-41-1), (b) grafted MCM-41 (MCM-41-2), (c) bipyridyl-functionalized MCM-41 (MCM-41-3) and (d) molybdenum-loaded MCM-41 (MCM-41-4).

value and a reduction of the pore size by the immobilized aminopropylsilyl groups. Functionalization of MCM-41-2 with bipyridyl groups and subsequent introduction of the complex $MoO_2Cl_2(THF)_2$ results in an expansion of the hexagonal unit cell, as revealed by the lattice parameters for MCM-41-3 (a = 41.6 Å) and MCM-41-4 (a = 42.3 Å). Three reflections are still observed for these two materials, indicating retention of the long-range hexagonal symmetry. It is evident, however, that the intensities of the (100), (110) and (200) reflections for MCM-41-4 are considerably reduced compared with the pristine host material MCM-41-1. This should not necessarily be interpreted as a severe loss of crystallinity.[9b] Instead, it is likely that there is a reduction in the X-ray scattering contrast between the silica wall and pore-filling material.[27,28] A similar phenomenon was observed for multiply-bonded dimolybdenum complexes grafted into MCM-41.[29]

N_2 adsorption–desorption isotherms. The low-temperature N_2 adsorption–desorption isotherm for the pristine MCM-41 sample (MCM-41-1) is shown in Fig. 2. It is of type IV as defined by IUPAC,[18] characteristic of mesoporous solids (pore width between 2 and 50 nm). The calculated textural parameters (S_{BET} = 1029 $m^2\ g^{-1}$, V_p = 0.81 $cm^3\ g^{-1}$) are in agreement with literature data.[30,31] The isotherm is completely reversible with no evidence of hysteresis resulting from capillary condensation/evaporation in the mesoporous media. A well-defined step is observed between relative pressures of 0.32 and 0.42, arising from the condensation of nitrogen inside the primary mesopores. The sharpness of this step reflects the uniform pore size. This is confirmed by the plot of differential volume as a function of pore size, which shows a very narrow pore size distribution (PSD). A value of 34 Å is obtained for the average pore diameter if this is taken as the maximum in the PSD curve.

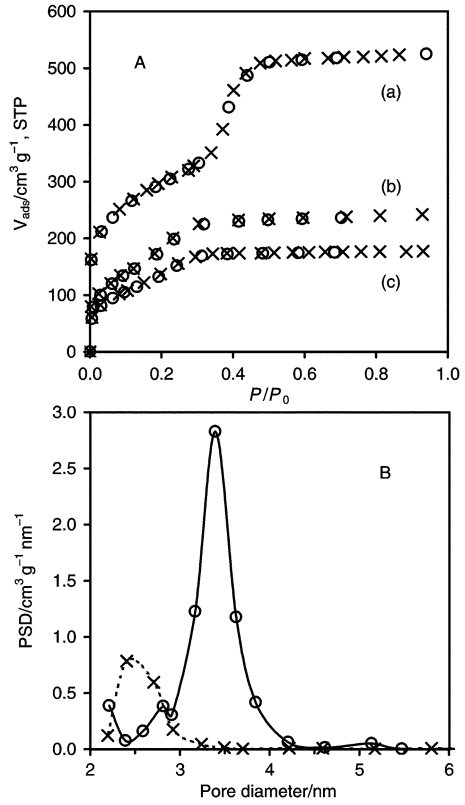

Fig. 2 A: N_2 adsorption (○) and desorption (×) isotherms at 77 K of (a) pristine MCM-41 (MCM-41-1), (b) bipyridyl-functionalized MCM-41 (MCM-41-3) and (c) molybdenum-loaded MCM-41 (MCM-41-4). B: Pore size distribution profiles for MCM-41-1 (———) and MCM-41-4 (·····).

Table 1 Textural parameters of MCM-41 samples determined from N_2 isotherms at 77 K

Sample	S_{BET}/ $m^2\ g^{-1}$	ΔS_{BET} (%)[a]	V_P/ $cm^3\ g^{-1}$	ΔV_P (%)[b]
MCM-41-1	1029	—	0.81	—
MCM-41-3	718	−30	0.37	−54
MCM-41-4	539	−48	0.27	−66

[a]Variation of surface area in relation to parent MCM-41-1. [b]Variation of total pore volume in relation to parent MCM-41-1.

The functionalized materials MCM-41-3 and MCM-41-4 also gave reversible type IV N_2 sorption isotherms indicating that the textural characteristics of the silica support are preserved during the grafting experiments and that the channels remain accessible (Fig. 2). Each of the modifications carried out to produce these two samples leads to a marked decrease in the limiting N_2 uptake at high p/p_0, and both the surface area and pore volume decrease (Table 1). The values obtained are comparable with other modified mesoporous silicas.[32] Furthermore, the height of the capillary condensation step, which is related to the volume of pore space confined by adsorbate film on the pore walls, is much smaller in the case of the modified MCM-41 materials. The p/p_0 coordinates of the inflection points of the isotherms decrease as MCM-41 is subsequently functionalized. This has previously been attributed to changes in pore size distribution due to immobilization of bulky complexes on the internal silica surface of MCM-41.[32] In fact, a comparison of the PSD curves for MCM-41-1 and MCM-41-4 reveals that the position of the maximum decreases from 34 to 24 Å. The decrease in the intensity of the maximum, together with an increase in the width at half height, indicates an increase in pore heterogeneity.

Solid-state MAS NMR studies. All samples were examined by solid-state ^{29}Si MAS and CP MAS NMR. Only the CP MAS results are included here. Pristine MCM-41 (MCM-41-1) displays two broad convoluted resonances in the ^{29}Si CP MAS NMR spectrum at δ = −109.5 and −100.3, assigned to Q^4 and Q^3 species of the silica framework, respectively, [Q^n = $Si(OSi)_n(OH)_{4-n}$] (Fig. 3, Table 2). A weak shoulder is also observed at δ = −91.3 for the Q^2 species. Grafting of the trimethoxysilane ligand into MCM-41 results in a reduction of the Q^3 and Q^2 resonances, and a concomitant increase of the Q^4 resonance. This is consistent with esterification of the isolated silanol groups (single and geminal) by nucleophilic substitution at the silicon atom in the organic ligand. Fig. 3 shows that there

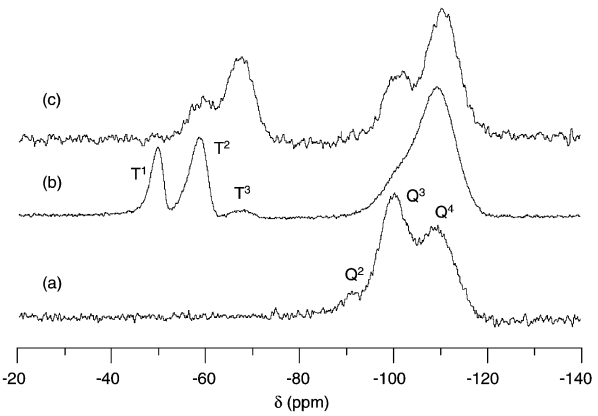

Fig. 3 ^{29}Si CP MAS NMR spectra of (a) pristine MCM-41 (MCM-41-1), (b) grafted MCM-41 (MCM-41-2) and (c) bipyridyl-functionalized MCM-41 (MCM-41-3).

Table 2 ^{29}Si and ^{13}C CP MAS NMR data for the MCM-41 materials (δ/ppm)

	MCM-41-1	MCM-41-2	MCM-41-3	MCM-41-4
$(O_3SiO)_{3-n}Si(OMe)_nCH_2R$	—	−49.8, −58.7, −68.1	−59.4, −67.7	−58.3, −67.5
$(O_3SiO)_3SiOH$	−100.3	—	−102.0	−101.4
$(O_3SiO)_4Si$	−109.5	−109.2	−110.0	−109.8
$Si(OMe)_nCH_2R$	—	49.3	48.6	47.6
$Si(OMe)_nCH_2R$	—	8.4	8.5	9.6
$Si(OMe)_nCH_2CH_2R$	—	25.9	25.8	25.0
$Si(OMe)_nCH_2CH_2CH_2Cl$	—	45.8	45.7	47.6
$Si(OMe)_nCH_2CH_2CH_2CH_2$-4′-Me-2,2′-bpy	—	—	34.4	35.4
$Si(OMe)_nCH_2CH_2CH_2CH_2$-4′-Me-2,2′-bpy	—	—	34.4	35.4
$Si(OMe)_nCH_2CH_2CH_2CH_2$-4′-*Me*-2,2′-bpy	—	—	20.7	22.2
$Si(OMe)_nCH_2CH_2CH_2CH_2$-4′-Me-2,2′-*bpy*	—	—	155.5, 148.8, 123.2	150.1, 123.3

are still unreacted Q^3 silicon atoms in MCM-41-2. These may be hydrogen-bonded silanols present at the surface, $(SiO)_3Si$–OH–OH–$Si(SiO)_3$, which have previously been shown to be unreactive to silylating agents.[23]

The ^{29}Si CP MAS NMR spectrum of MCM-41-2 also displays two signals at $\delta = -49.8$ and -58.7, assigned to T^1 and T^2 organosilica species, respectively, [$T^m = RSi(OSi)_m(OMe)_{3-m}$]. A weak, broad signal at $\delta = -68.1$ is assigned to a T^3 environment. The ^{13}C CP MAS NMR spectrum of MCM-41-2 exhibits one peak at $\delta = 49.3$ attributed to residual methoxide groups, and three sharp peaks at $\delta = 45.8$, 25.9 and 8.4 attributed to the methylene carbons of the surface-bound spacer ligand (Fig. 4, Table 2). In agreement with elemental analysis, both the ^{29}Si and ^{13}C NMR spectra indicate that monopodal and bipodal anchoring of the organic ligand predominate.

Coupling of the bipyridine ligand to MCM-41-2 resulted in significant changes to the signals for the organosilica species in the ^{29}Si CP MAS NMR spectrum (Fig. 3). The relative intensity of the T^3 resonance is markedly enhanced in the spectrum of MCM-41-3 compared with MCM-41-2, which suggests that the alkoxysilane underwent further condensation on the silica surface during the reaction. Probably the pyridyl groups and also diisopropylamine enhance the substitution reaction at the Si atom. This effect has been observed previously with MCM-41 grafted with (3-aminopropyl)trialkoxysilane,[32] and amines such as triethylamine are well known to activate surface silanols for derivatization reactions.[33] The ^{13}C CP MAS NMR spectrum of MCM-41-3 verifies the presence of covalently tethered bipyridyl groups (Fig. 4). The broad peaks at $\delta = 155.5$, 148.8 and 123.2 are readily assigned to pyridyl ring carbons (Table 2). In addition, two broad peaks are observed at $\delta = 34.4$ and 20.7. The first of these does not appear in the spectra of either MCM-41-2 or 4,4′-dimethyl-2,2′-bipyridine. It is assigned to the two methylene carbons –CH_2CH_2–bpy and confirms that the coupling reaction worked.

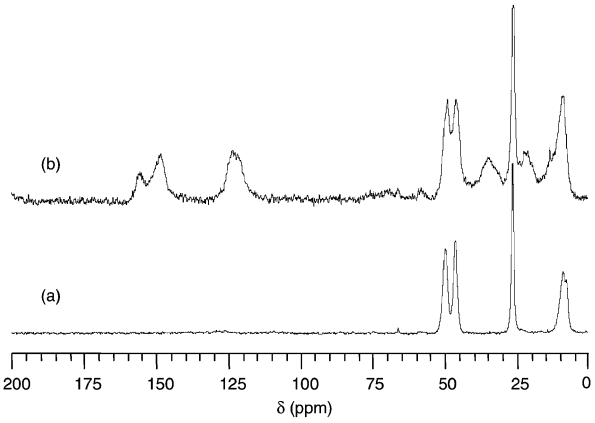

Fig. 4 ^{13}C CP MAS NMR spectra of (a) grafted MCM-41 (MCM-41-2) and (b) bipyridyl-functionalized MCM-41 (MCM-41-3).

In order to be sure about this assignment, the model compound 4-(n-butyl)-4′-methyl-2,2′-bipyridine was prepared using the method of Ellison and Iwamoto.[17] The ^{13}C spectrum of this ligand ($CDCl_3$) contains signals at $\delta = 35.2$ and 32.5 assigned to –CH_2–bpy and –CH_2CH_2–bpy, respectively.[34] The 4′-methyl group appears at $\delta = 21.2$ and therefore the peak at $\delta = 20.7$ in the spectrum of MCM-41-3 is assigned likewise. There are unreacted chloropropyl groups in MCM-41-3, as evidenced by the signal at $\delta = 45.7$ (–CH_2Cl), and the signal at $\delta = 48.6$ confirms that there are residual methoxy groups.

The ^{29}Si and ^{13}C CP MAS NMR spectra of molybdenum-containing MCM-41-4 were not significantly different from that of MCM-41-3 (Table 2).

EXAFS studies. Mo K-edge XAFS studies were carried out in the solid-state at room temperature in order to characterize the average local environment of molybdenum centers in MCM-41-4. The complexes $MoO_2Cl_2(THF)_2$ (**1**) and MoO_2Cl_2(4,4′-dimethyl-2,2′-bipyridine) (**2**) were measured as model compounds (Chart 1). It was anticipated that a ligand exchange reaction would take place upon treatment of MCM-41-3 with a CH_2Cl_2 solution of **1**, leading to the formation of a tethered Lewis base adduct analogous to **2**. This method is generally applicable to the synthesis of complexes of the type MoO_2X_2L (L = bidentate *N*,*O*-ligand).[16] However, MCM-41-3 exhibited an unexpectedly high encapsulating ability (see above) and elemental analysis indicated a metal : ligand ratio of 3.6 : 1 in MCM-41-4. This was an initial indication that other immobilized species were formed in addition to, or instead of, the desired complex.

The Mo K-edge EXAFS of $MoO_2Cl_2(THF)_2$ was fitted by three shells corresponding to Mo–$O_{terminal}$, Mo–O_{THF} and Mo–Cl (Fig. 5, Table 3). In the case of the bipyridine adduct **2**, four shells were included for O, N, Cl and C neighbors, in order of increasing distance from the absorbing atom. The refined distances and coordination numbers for **2** are in good agreement with the expected structure (Table 3).[36] In the case of MCM-41-4, the presence of *cis*-MoO_2 units was confirmed by modeling two oxygen atoms at 1.69 Å. A shell for chlorine atoms was also found at 2.37 Å, although the best coordination number for this shell was only 0.5. This result is somewhat at odds with elemental analysis which suggests a Mo : Cl stoichiometry of 1 : 2 for the included molybdenum species. The Fourier transform of the Mo K-edge EXAFS of MCM-41-4 clearly indicates the presence of a third significant shell above 3 Å. This was best fitted with one molybdenum atom at 3.28 Å.

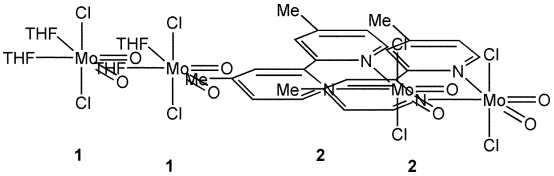

Chart 1

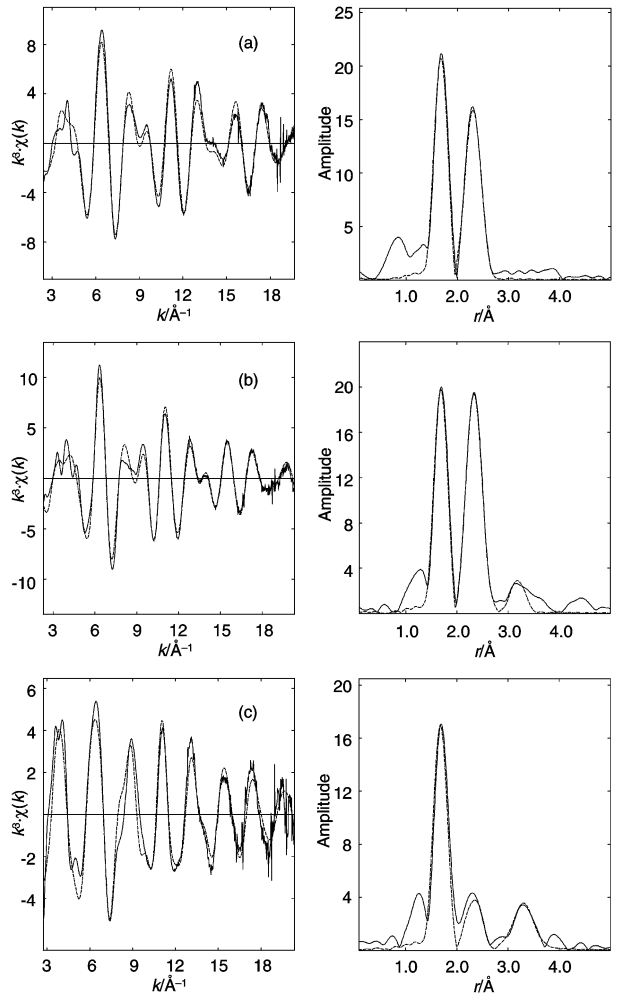

Fig. 5 Room-temperature solid-state Mo K-edge EXAFS and Fourier transforms of (a) $MoO_2Cl_2(THF)_2$, (b) MoO_2Cl_2(4,4′-dimethyl-2,2′-bipyridine) and (c) MCM-41-4. The solid lines represent the experimental data and the dashed lines show the best fits using the parameters given in Table 3.

Obviously, the existence of this shell suggests that a large fraction if not all of the molybdenum species in MCM-41-4 comprises Mo_2 dimers, most likely unidentate-bridged entities of the type Mo–X–Mo. The existence of such species was further indicated by the fact that an improvement in the fit was obtained upon addition of a fourth shell of oxygen atoms at 1.97 Å, corresponding to Mo–O bridging.[37] No acceptable fit to the EXAFS could be obtained for a shell of nitrogen atoms between 2.2 and 2.4 Å, and therefore coordination of bipyridyl groups to molybdenum centers cannot be confirmed. It seems likely that the molybdenum species in MCM-41-4 are analogous to the supported oxybridged bimetallic species obtained after immobilization of $MoO_2(acac)_2$ in polymer supports carrying hydroxypropylaminomethyl pyridine ligands.[25]

Catalytic epoxidation

The oxidation of cyclooctene in the presence of MCM-41-4, using TBHP as oxidant at 55 °C, yields cyclooctene oxide as the only product. Without a catalyst the reaction does not take place. Initial activity for cyclooctene oxidation is 40.6 mmol g cat.$^{-1}$ h^{-1}, which is much higher than that observed with MCM-41-1 or MCM-41-3 (less than 1 mmol g cat.$^{-1}$ h^{-1}) under identical reaction conditions (Table 4). These results suggest that the active centers for epoxidation are mainly molybdenum-containing species. The kinetic profile for MCM-41-4 shows a high initial reaction rate followed by a sudden decrease in activity (Fig. 6), similar to that found previously for MoO_2Cl_2 complexes tethered to MCM-41 *via* monodentate nitrile ligands.[24] The slowdown in activity with reaction time is probably due to the formation of *tert*-butanol, which acts as a competitive inhibitor for the attack of TBHP at the molybdenum center. For comparison, the reaction was also carried out under homogeneous conditions using complex **2** as the catalyst precursor (1% molar ratio of complex/cyclooctene). Once again, only the epoxide was produced. Fig. 6 shows that, as observed for the supported complex, the reaction is fast at the beginning (initial activity 93.3 mmol g cat.$^{-1}$ h^{-1}) but then slows down somewhat.

The lifetime of MCM-41-4 was examined by using it in a second reaction cycle. Before reuse the solid was separated from the reaction medium by filtration, washed with dichloromethane and finally dried at 40 °C. Cyclooctene conversion

Table 4 Cyclooctene oxidation using TBHP in the presence of MCM-41 materials and complex MoO_2Cl_2(4,4′-dimethyl-2,2′-bipyridine) (**2**)

Sample	Initial activity[a]/mmol g cat.$^{-1}$ h^{-1}	Conv.[b] (%)	Selectivity to cyclooctene oxide (%)
MCM-41-1	0.8	18.6	91.0[c]
MCM-41-3	0.3	13.6	100
MCM-41-4 (1st run)	40.6	74.1	100
MCM-41-4 (2nd run)[d]	0.3	45.4	94.8[c]
2	93.3	97.1	100

[a]Calculated as [mmol converted substrate/(mmol catalyst × 0.25 h)]. [b]Cyclooctene conversion after 24 h. [c]1,2-Cyclooctanediol was formed. [d]Carried out after filtration of the first run, washing with dichloromethane and drying at 40 °C.

Table 3 Mo K-edge EXAFS-derived structural parameters for $MoO_2Cl_2(THF)_2$ (**1**), MoO_2Cl_2(4,4′-dimethyl-2,2′-bipyridine) (**2**) and MCM-41-4

Compound	Atom	CN[a]	r/Å	$2\sigma^2$/Å$^{2\,b}$	E_f/eV[c]	R (%)[d]
1	O	2.0(1)	1.691(2)	0.0023(2)	1.7(7)	26.7
	O	2.0(9)	2.254(16)	0.0286(71)		
	Cl	1.8(2)	2.351(3)	0.0053(3)		
2[e]	O	2.0(1)	1.698(1)	0.0026(2)	−0.1(5)	22.9
	N	1.7(3)	2.298(9)	0.0038(15)		
	Cl	2.5(2)	2.372(3)	0.0079(9)		
	C	4.2(8)	3.206(10)	0.0095(19)		
MCM-41-4	O	1.9(1)	1.694(2)	0.0033(2)	7.9(7)	32.5
	Cl	0.5(1)	2.365(7)	0.0055(12)		
	Mo	1.0(4)	3.280(8)	0.0122(13)		

[a]CN = Coordination number. Values in parentheses are statistical errors generated in EXCURVE. The true errors in coordination numbers are likely to be of the order of 20%; those for the interatomic distances *ca.* 1.5%.[35] [b]Debye–Waller factor; σ = root-mean-square internuclear separation. [c]E_f = edge position (Fermi energy), relative to calculated vacuum zero. [d]$R = (\int[\Sigma^{theory} - \Sigma^{exptl}]k^3 dk/[\Sigma^{exptl}]k^3 dk) \times 100\%$. [e]Crystallographic bond distances:[36] Mo–O = 1.696, 1.695 Å; Mo–N = 2.310, 2.304 Å; Mo–Cl = 2.375, 2.370 Å.

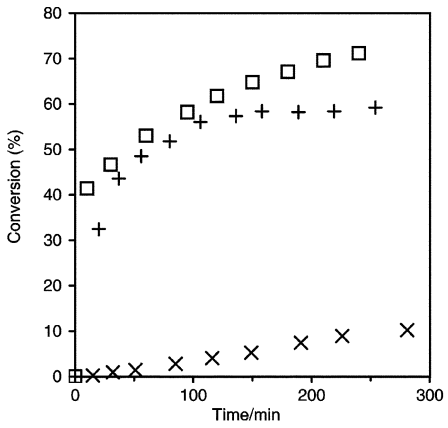

Fig. 6 Cyclooctene conversion profiles for epoxidation reactions carried out at 55 °C with TBHP as oxidant. Catalyst precursors are MoO_2Cl_2(4,4′-dimethyl-2,2′-bipyridine) **2** (□) and MCM-41-4 (+, first run; ×, second run).

decreased significantly and initial activity was comparable to that of the MCM-41 materials without molybdenum, *i.e.* less than 1 mmol g cat.$^{-1}$ h^{-1} (Fig. 6, Table 4). Selectivity to cyclooctene oxide decreased slightly due to the formation of 1,2-cyclooctanediol, which was also produced with pristine MCM-41. Catalyst deactivation may be due to leaching of molybdenum species from the solid to solution during oxidation, which may contribute to the observed catalytic activity. In order to confirm this, the catalytic reaction with fresh MCM-41-4 was repeated, but this time the reaction mixture was filtered after 20 min (at which point the conversion of cyclooctene was *ca.* 32%). The filtrate was then allowed to react for a further 280 min at 55 °C. The conversion of cyclooctene obtained was 60%, which is very similar to that obtained without the filtration step (Fig. 6). A small amount (<1%) of 1,2-cyclooctanediol was also formed. These results suggest that epoxidation in the presence of MCM-41-4 is, at least to a certain extent, homogeneously catalyzed by leached molybdenum species.

The filtered solid from the above leaching test was characterized by elemental analysis (Mo, C and N) and FTIR spectroscopy. The IR spectrum in the range 400–1500 cm^{-1}, comprising bands due to the silica host and also the Mo=O stretching vibrations, was very similar to that of the precursor MCM-41-4. This suggests that the material was largely unchanged by the catalytic reaction, especially concerning the tethered bipyridyl ligands. Elemental analysis confirmed only a small decrease in the molybdenum content ($\leqslant 5$%). The leached molybdenum species probably originate from the immobilized dimeric species, which are weakly bound to the lattice.[38] It is likely that the Mo–O–Mo bridge is cleaved by reaction with TBHP, yielding catalytically active mononuclear species in solution. This phenomenon has been reported previously for alkene epoxidations catalyzed by certain polymer-supported oxomolybdenum complexes.[25]

Conclusions

We have reported a new method for the functionalization of mesoporous silica (MCM-41) with unsymmetrical 4,4′-dialkyl-2,2′-bipyridyl groups without loss of the regular pore structure. Only about one fifth of the chloropropyl groups in the precursor grafted material could be converted. The coordination chemistry of the ligand-silica was studied for the formation of dioxomolybdenum(VI) complexes in a constrained environment. However, the material has a very high encapsulating ability and the presence of an immobilized complex of the type MoO_2Cl_2(bpy) could not be proven. Instead, oxo-bridged dimers were formed, probably as a result of the high metal loading. This undoubtedly explains the disappointing results obtained in catalytic alkene epoxidations. It may be that the use of lower metal loadings will result in more strongly bound monomeric complexes. The ability of the ligand-silica to bind other transition metals, *e.g.* Fe and Mn, is also of interest. These studies are currently underway in our laboratories.

Acknowledgements

The authors are grateful to FCT, POCTI and FEDER for financial support (Project PCTI/1999/QUI/32889). A. A. V. and M. P. thank FCT for post-doctoral grants, and C. D. N. thanks the University of Aveiro for a research grant. We acknowledge the European Synchrotron Radiation Facility for provision of synchrotron radiation facilities and we would like to thank Stuart Ansell for assistance in using beamline BM29. Marta Lopes and Cláudia Morais are acknowledged for assistance in the NMR experiments.

References

1 Y. Iwasawa, in *Tailored Metal Catalysts*, ed. Y. Iwasawa, D. Riedel, Dordrecht, 1986, pp. 1–85.
2 U. Deschler, P. Kleinschmit and P. Panster, *Angew. Chem., Int. Ed. Engl.*, 1986, **25**, 236.
3 R. D. Hancock, I. V. Howell, R. C. Pitkethly and P. J. Robinson, in *Catalysis: Heterogeneous and Homogeneous, Proceedings of the International Symposium on the Relations between Heterogeneous and Homogeneous Catalytic Phenomena*, B. Delmon and G. Jannes, ed., Elsevier, Amsterdam, 1975, pp. 361–371.
4 K. G. Allum, R. D. Hancock, I. V. Howell, S. McKenzie, R. C. Pitkethly and P. J. Robinson, *J. Organomet. Chem.*, 1975, **87**, 203.
5 K. G. Allum, R. D. Hancock, I. V. Howell, T. E. Lester, S. McKenzie, R. C. Pitkethly and P. J. Robinson, *J. Organomet. Chem.*, 1976, **107**, 393.
6 H. Yang, H. Gao and R. J. Angelici, *Organometallics*, 1999, **18**, 2285; H. Yang, H. Gao and R. J. Angelici, *Organometallics*, 2000, **19**, 622.
7 J. Y. Ying, C. P. Mehnert and M. S. Wong, *Angew. Chem., Int. Ed.*, 1999, **38**, 56.
8 C. T. Kresge, M. E. Leonowicz, W. J. Roth, J. C. Vartuli and J. S. Beck, *Nature*, 1992, **359**, 710; J. S. Beck, J. C. Vartuli, W. J. Roth, M. E. Leonowicz, C. T. Kresge, K. D. Schmitt, C. T.-W Chu, D. H. Olson, E. W. Sheppard, S. B. McCullen, J. B. Higgins and J. L. Schlenker, *J. Am. Chem. Soc.*, 1992, **114**, 10 834.
9 (*a*) K. Moller and T. Bein, *Chem. Mater.*, 1998, **10**, 2950; (*b*) T. Maschmeyer, *Curr. Opin. Solid State Mater. Sci.*, 1998, **3**, 71.
10 D. Brunel, N. Bellocq, P. Sutra, A. Cauvel, M. Laspéras, P. Moreau, F. DiRenzo, A. Galarneau and F. Fajula, *Coord. Chem. Rev.*, 1998, **178–180**, 1085; D. Brunel, *Microporous Mesoporous Mater.*, 1999, **27**, 329.
11 A. Corma, *Chem. Rev.*, 1997, **97**, 2373; A. Sayari, *Chem. Mater.*, 1996, **8**, 1840.
12 S.-S. Kim, W. Zhang and T. J. Pinnavaia, *Catal. Lett.*, 1997, **43**, 149; Z. Luan, J. Xu and L. Kevan, *Chem. Mater.*, 1998, **10**, 3699.
13 S. Zheng, L. Gao and J.-K. Guo, *J. Inorg. Mater.*, 2000, **15**, 1015; Y. X. Jiang, W. B. Song and H. D. Xu, *Mater. Chem. Phys.*, 2000, **62**, 109; K. Fujishima, A. Fukuoka, A. Yamagishi, S. Inagaki, Y. Fukushima and M. Ichikawa, *J. Mol. Catal. A: Chem.*, 2001, **166**, 211; M. Ogawa, T. Nakamura, J. Mori and K. Kuroda, *J. Phys. Chem. B*, 2000, **104**, 8554.
14 R. Colton and I. B. Tomkins, *Aust. J. Chem.*, 1965, **18**, 447.
15 W. M. Carmichael, D. A. Edwards, G. W. A. Fowles and P. R. Marshall, *Inorg. Chim. Acta*, 1967, **1**, 93.
16 F. E. Kühn, A. D. Lopes, A. M. Santos, E. Herdtweck, J. J. Haider, C. C. Romão and A. G. Santos, *J. Mol. Catal. A: Chem.*, 2000, **151**, 147.
17 D. K. Ellison and R. T. Iwamoto, *Tetrahedron Lett.*, 1983, **24**, 31.
18 S. J. Gregg and K. S. W. Sing, *Adsorption, Surface Area and Porosity*, Academic Press, London, 2nd edn., 1982.
19 J. M. Thomas and W. J. Thomas, *Principles and Practices of Heterogeneous Catalysis*, VCH, Weinheim, 1997.
20 M. R. Bhambhani, P. A. Cutting, K. S. W. Sing and D. H. Turk, *J. Colloid Interface Sci.*, 1972, **38**, 109.

21 N. Binsted, EXCURV98, CCLRC Daresbury Laboratory computer programme, 1998.
22 S. J. Gurman, N. Binsted and I. Ross, *J. Phys. C*, 1984, **17**, 143; S. J. Gurman, N. Binsted and I. Ross, *J. Phys. C*, 1986, **19** 1845.
23 X. S. Zhao, G. Q. Lu, A. K. Whittaker, G. J. Miller and H. Y. Zhu, *J. Phys. Chem. B*, 1997, **101**, 6525.
24 P. Ferreira, I. S. Gonçalves, F. E. Kühn, A. D. Lopes, M. A. Martins, M. Pillinger, A. Pina, J. Rocha, C. C. Romão, A. M. Santos, T. M. Santos and A. A. Valente, *Eur. J. Inorg. Chem.*, 2000, 2263.
25 D. C. Sherrington, *J. Catal.*, 1995, **152**, 368; M. M. Miller and D. C. Sherrington, *J. Catal.*, 1995, **152**, 377.
26 W. A. Carvalho, M. Wallau and U. Schuchardt, *J. Mol. Catal. A: Chem.*, 1999, **144**, 91.
27 B. Marler, U. Oberhagemann, S. Voltmann and H. Gies, *Microporous Mater.*, 1996, **6**, 375.
28 W. Hammond, E. Prouzet, S. D. Mahanti and T. J. Pinnavaia, *Microporous Mesoporous Mater.*, 1999, **27**, 19.
29 P. Ferreira, I. S. Gonçalves, F. E. Kühn, M. Pillinger, J. Rocha, A. Thursfield, W. M. Xue and G. Zhang, *J. Mater. Chem.*, 2000, **10**, 1395.
30 M. D. Alba, A. Becerro and J. Klinowski, *J. Chem. Soc., Faraday Trans.*, 1996, **92**, 849.
31 A. A. Romero, M. D. Alba, W. Zhou and J. Klinowski, *J. Phys. Chem. B*, 1997, **101**, 5294.
32 D. Brunel, A. Cauvel, F. Fajula and F. DiRenzo, *Stud. Surf. Sci. Catal.*, 1995, **97**, 173.
33 T. Maschmeyer, F. Rey, G. Sankar and J. M. Thomas, *Nature*, 1995, **378**, 159.
34 ^{13}C NMR of 4-(n-butyl)-4′-methyl-2,2′-bipyridine ($CDCl_3$, r.t., 75.47 MHz, TMS): δ = 156.0, 152.9, 148.9, 124.6, 123.9, 122.0, 121.3, 35.2, 32.5, 22.4, 21.2, 13.9.
35 J. Evans, J. T. Gauntlett and J. F. W. Mosselmans, *Faraday Discuss. Chem. Soc.*, 1990, **89**, 107.
36 D. M. Baird, F. L. Yang, D. J. Kavanaugh, G. Finness and K. R. Dunbar, *Polyhedron*, 1996, **15**, 2597.
37 Fourth oxygen shell: Mo–O = 1.965(13) Å, $2\sigma^2$ = 0.0094(29) Å^2, CN = 0.6(2), R = 31.2%. The structural parameters for the other three shells were largely unchanged compared to those for the three-shell model given in Table 3.
38 I. J. Shannon, T. Maschmeyer, R. D. Oldroyd, G. Sankar, J. M. Thomas, H. Pernot, J.-P. Balikdjian and M. Che, *J. Chem. Soc., Faraday Trans.*, 1998, **94**, 1495.